Eur Radiol (2010) 20: 1985–1993
DOI 10.1007/s00330-010-1751-5

INTERVENTIONAL

Jens Ricke
Markus Thormann
Matthias Ludewig
Kerstin Jungnickel
Oliver Grosser
Christian Wybranski
Nils Peters
Peter Hass
Jürgen Bunke
Frank Fischbach

MR-guided liver tumor ablation employing open high-field 1.0T MRI for image-guided brachytherapy

Received: 4 November 2009
Revised: 21 December 2009
Accepted: 15 January 2010
Published online: 20 March 2010

J. Ricke (✉) · M. Thormann · M. Ludewig · K. Jungnickel · O. Grosser · C. Wybranski · F. Fischbach
Klinik für Radiologie und Nuklearmedizin, Universitätsklinikum Magdeburg AöR, Leipzigerstrasse 44, 39120 Magdeburg, Germany
e-mail: jens.ricke@med.ovgu.de

N. Peters · P. Hass
Klinik für Strahlentherapie, Universitätsklinikum Magdeburg AöR, Magdeburg, Germany

J. Bunke
Philips Healthcare, Hamburg, Germany

Abstract *Objective:* To determine the feasibility and safety of image-guided brachytherapy employing a modified open high-field MR system. *Methods:* This is a follow-up study of a development project enabling technologies for interventional use of 1.0T open MRI. Modifications included coils and in-bore visualization, fluoroscopic sequences and user interfaces. We recruited 104 patients with 224 liver malignancies to receive MR-guided brachytherapy. Interventions were performed >20 min after Gd-EOB-DTPA. We recorded interventional parameters including the intervention time (from acquisition of the first scout until the final sequence for brachytherapy treatment planning). Two reviewers assessed MR-fluoroscopic images in comparison to plain CT as used in CT intervention, applying a rating scale of 1–10. Statistical analysis included Friedman and Kendall's W tests. *Results:* We employed freehand puncture with interactive dynamic imaging for navigation. Technical success rate was 218 complete ablations in 224 tumours (97%). The median intervention time was 61 min. We recorded no adverse events related to the use of MRI. No major complications occurred. The rate of minor complications was 4%. Local control at 3 months was 96%. Superiority of MR-fluoroscopic, Gd-EOB-DTPA-enhanced images over plain CT was highly significant ($P<0.001$). *Conclusion:* MR-guided brachytherapy employing open high-field MRI is feasible and safe.

Key words MR intervention · Liver malignancies · Brachytherapy · Minimally invasive oncology

Introduction

Percutaneous ablative therapies achieve substantial tumour kill by directly applying chemicals, temperature changes or radiation to solid tumours, and they are most widely accepted for their application in the treatment of liver tumours [1–5]. In comparison to traditional cancer treatments, these image-guided ablation techniques offer the advantage of reduced morbidity and mortality, as well as lower procedural costs when compared with traditional surgical methods. They can also be performed on an outpatient basis, repeated over time, or combined with other anticancer treatments. Their intention is usually palliative, even though some authors claim a curative potential based on retrospective data [6].

The key to optimum local treatment success is the accuracy of image guidance. To enable access to liver tumours, ultrasound or computed tomography are most commonly used. However, limitations apply for both methods: in liver malignancies a lack of lesion-to-liver contrast is frequent [specifically when applying computed tomography (CT)], and there are technical limitations to visualizing the tumour and the access to it in lesions located close to the liver hilum or in the liver dome [7–11]. In addition, treatment success in, for example, radiofrequency (RF) ablation is directly correlated with accurate needle placement, which is often difficult to achieve in a single

plane only, as is provided in computed tomography (CT). When applying ultrasound for RFA guidance, the probe and its antennas might often be difficult to visualize during placement, and gas formation due to heating of tissue frequently leads to severe imaging limitations [12]. In image-guided brachytherapy, dosimetry can only be calculated based on 3D image data, such as generated by CT or magnetic resonance imaging (MRI) [13].

Several research groups have developed and evaluated solutions employing MRI in liver tumour treatments. Some groups limited themselves to using MRI with cylindrical magnet configurations for verification of the probe position after ultrasound- or CT-guided probe placement, sometimes supplemented by thermal monitoring specifically in laser-induced ablation [14, 15]. Other groups have tested closed bore high-field MRI for image-guided needle placement. However, in these systems access to the patient is severely limited and needle repositioning has to be performed outside of the magnet with intermittent acquisition of images [16]. Finally, open low-field MRI has been tested for MR fluoroscopy in liver intervention, but image quality has never been acceptable, and these interventions have not translated into routine clinical use [17–20].

In recent years, open MR systems with high-field strength such as 1.5T (employing a short magnet with a wide opening) or, as applied by our own workgroup, 1.0T have been introduced. The latter magnet is configured in a doughnut design, using two superconductive coils as part of a yoke to generate a vertical magnetic field with specific challenges and opportunities [21, 22].

In the exploratory study described herein, we assessed the clinical use of this magnet for liver tumour ablation by image-guided brachytherapy. This is a follow-up study of a 1-year development project that served to enable technologies for interventional use with this machine, including hardware and software modifications such as development of coils, in-bore visualization, MR imaging sequences for fluoroscopy, and user interfaces as well as preclinical assessment of safety and feasibility of needles, guide wires and catheters to be used in a 1.0T magnet. We report the results of 104 patients with 224 liver malignancies undergoing 134 sessions of image-guided brachytherapy in an open high-field MRI system.

Materials and methods

Study design

We performed an exploratory retrospective analysis of feasibility and safety of local ablation by image-guided brachytherapy in 1.0T open high-field MRI. The technical setup including hardware and software, configuration of the magnet, coil development, safety and feasibility assessments of the tools and catheters employed, as well as sequence design for MR fluoroscopy were a result of a continued joint development project between our work group and Philips Healthcare. We included patients treated with MR-guided brachytherapy at our institution between February 2008 and February 2009. At this time, the following features had entered clinical routine status as a result of previous development and evaluation activities: an optimised surface coil for intervention, fluoroscopic MR sequences optimised for liver lesion contrast after i.v. Primovist, in-bore visualization of images, a foot pedal for assisted modification of the image orientation during continuous imaging, brachytherapy sheath and catheter, puncture needle and guide wire. Primary endpoints of the analysis were safety and feasibility.

The study was approved by the local ethics committee, and written informed consent was obtained from all patients.

Patients

Patients with either histologically confirmed primary or secondary liver malignancies or hepatocellular carcinoma (HCC) diagnosis according to AASL criteria were eligible to participate in this study. For the exploration of the method, a maximum lesion size of 4 cm was applied in the first patients. However, as brachytherapy generally is not limited by tumour size, patients with larger tumours were included as our experience with MR guidance increased [23]. We excluded patients with five or more lesions. Extrahepatic tumour spread was not an exclusion criterion, and the decision to treat these patients was made in interdisciplinary consensus based on individual considerations including the histopathology of the primary tumour as well as the actual staging and previous therapies. Additional eligibility criteria included preserved liver function with bilirubin <3 mg/dl and a PT>50%, preserved haematological function with a platelet count of >50,000/mm^3, Karnofsky index ≥70% and ECOG 0–2.

Interventional technique for catheter implantation employing open high-field MRI

Patients received 0.1 ml/kg body weight of a 0.25 mol/L (181.43 mg/ml) solution of gadoxetic acid disodium (Gd-EOB-DTPA, Primovist, BayerSchering, Germany). Primovist is a paramagnetic liver-specific contrast agent. As a result of hepatocyte uptake, normal liver parenchyma exhibits T1 shortening leading to an increase in signal intensity on T1-weighted images, whereas malignant focal liver lesions do not exhibit T1 shortening. This increases image contrast and thus lesion conspicuity compared with plain investigations. Peak liver signal intensities are seen 15–20 min after injection followed by a plateau of constant signal intensities for approximately 2 h. This extended

imaging window provides ample time for minimally invasive liver interventions [24, 25].

We used a ceramic scalpel (SLC Ceramic, Germany) for the skin incision and an 18-gauge MR-compatible puncture needle with a length of 150 or 200 mm (Invivo, Germany). For exchange of the needle versus an angiography sheath (6F, Terumo, Japan), we employed a standard 0.0035-in hydrophilic angiographic guide wire with a nitinol core (Terumo, Japan). The exchange was performed using the Seldinger technique outside the magnet without simultaneous imaging.

Magnetic resonance guidance was performed using a 1.0T imaging system (Panorama, Philips Healthcare). A ring-shaped 21-cm-diameter surface loop receive-only coil developed as part of the project was used for signal reception and placed in the region of the liver over the area of interest. The coil provides depth coverage approximately equal to the diameter of the closed ring.

For visualization of the fluoroscopic images for the interventionalist, both an in-room RF-shielded liquid crystal monitor (Philips Healthcare, the Netherlands) as well as a projection system employing a shield of sanded glass inside the magnet serving as a screen for a beamer positioned outside the RF cage were used.

A USB foot switch (Herga Electric, United Kingdom) was connected to a USB socket to simulate keystrokes necessary to steer the interactive imaging mode of the device. With this foot switch, the interventionalist switched between two imaging planes adapted online to the procedural progress by an MR technician in the control room.

To perform the procedure, the patient was placed in supine position. Depending on the intended percutaneous access route and the position of the target inside the liver, the patient position was rotated up to 30° towards a lateral decubitus position on occasion. This manoeuvre helped to optimise the presumed angle between needle and the vertical B_0 for improved conspicuity of the needle because of susceptibility effects. Following the results of pretests using MR phantoms, we allowed an angle ≥30° between the puncture needle and B_0 despite the fact that the needle artefact is most prominent with a needle position perpendicular to B_0.

To determine the position of the target lesion at the beginning of the intervention, breath hold static transversal images of the liver were obtained with a T1-weighted, fat signal-saturated 3D high resolution isotropic volume examination (THRIVE) with a flip angle of 12°, a repetition (TR) of 5.4 ms and an echo time (TE) of 2.6 ms. A voxel size of 1.5 x 2 mm and a slice thickness of 3 mm were adjusted. Sixty-five slices in a breath-hold time of 17 s were sufficient to cover most of the livers investigated.

The skin entry site was defined with finger pointing in an interactive mode with fast dynamic imaging using a T1-weighted gradient echo sequence (T1 FFE) with a flip angle of 35°, a repetition (TR) of 11 ms and an echo time (TE) of 6 ms. A voxel size of 2 x 2.4 mm and a slice thickness of 8 mm were adjusted producing images with a clinically adequate signal-to-noise ratio. Fluoroscopic images were acquired with 1.1 s per frame (Fig. 1a–h).

To guide the interventionalist, two perpendicular planes were defined, both displaying the skin entry point as well as the target position. As a result, disappearance of the needle tip caused by deviation from the intended path upon needle progression in interactive continuous imaging mode could be corrected by alternating between the two fluoroscopic imaging planes using the foot switch. After final positioning of the needle, the patient was moved out of the magnet and the needle was replaced by the angiography sheath using the Seldinger technique. The brachytherapy catheters were then positioned in the sheath with a Terumo guide wire shortened to 38 cm inside to allow visualization of the catheter position during a final THRIVE acquisition for treatment planning.

Irradiation technique

The technique of image-guided brachytherapy (employing CT) has been described in detail elsewhere [13]. Generally, one catheter per 1–2 cm of tumour diameter was implanted. For treatment planning purposes, the final THRIVE data set was transferred to the treatment planning system (Oncentra-MasterPlan, BrachyModul, Nucletron, the Netherlands). This planning system was used to determine the relative coordinates (x, y, z) of the catheters as well as the tumour boundaries manually. The HDR afterloading system (microSelectron Digital V3, Nucletron, the Netherlands) used a ^{192}Iridium source of 10 Ci. The source diameter was <1 mm. Based on previous assessments, the minimum target dose prescribed was 15 Gy for HCC, breast cancer and squamous cell cancer (laryngeal or bronchial origin), and 20 Gy for colorectal and all other primaries. The duration of the irradiation was typically 20–40 min.

A dose exposure of 5 Gy to more than two-thirds of the liver served as a prospective constraint. Maximum exposure to stomach, duodenum or colon was set at 15 Gy/ml of organ surface, and 8 Gy/ml for the spinal cord. After irradiation, a gastric prophylaxis (pantoprazole 1 x 40 mg/day for 3 months and magaldrate H_2O-free on demand) was prescribed if the gastric or duodenal mucosa was calculated to have received more than 10 Gy/ml. No potentially protective measures against radiation hepatitis such as cortisone or anticoagulants were applied.

Assessments

Adverse events related to the procedure as well as late toxic effects were graded according to the National Cancer

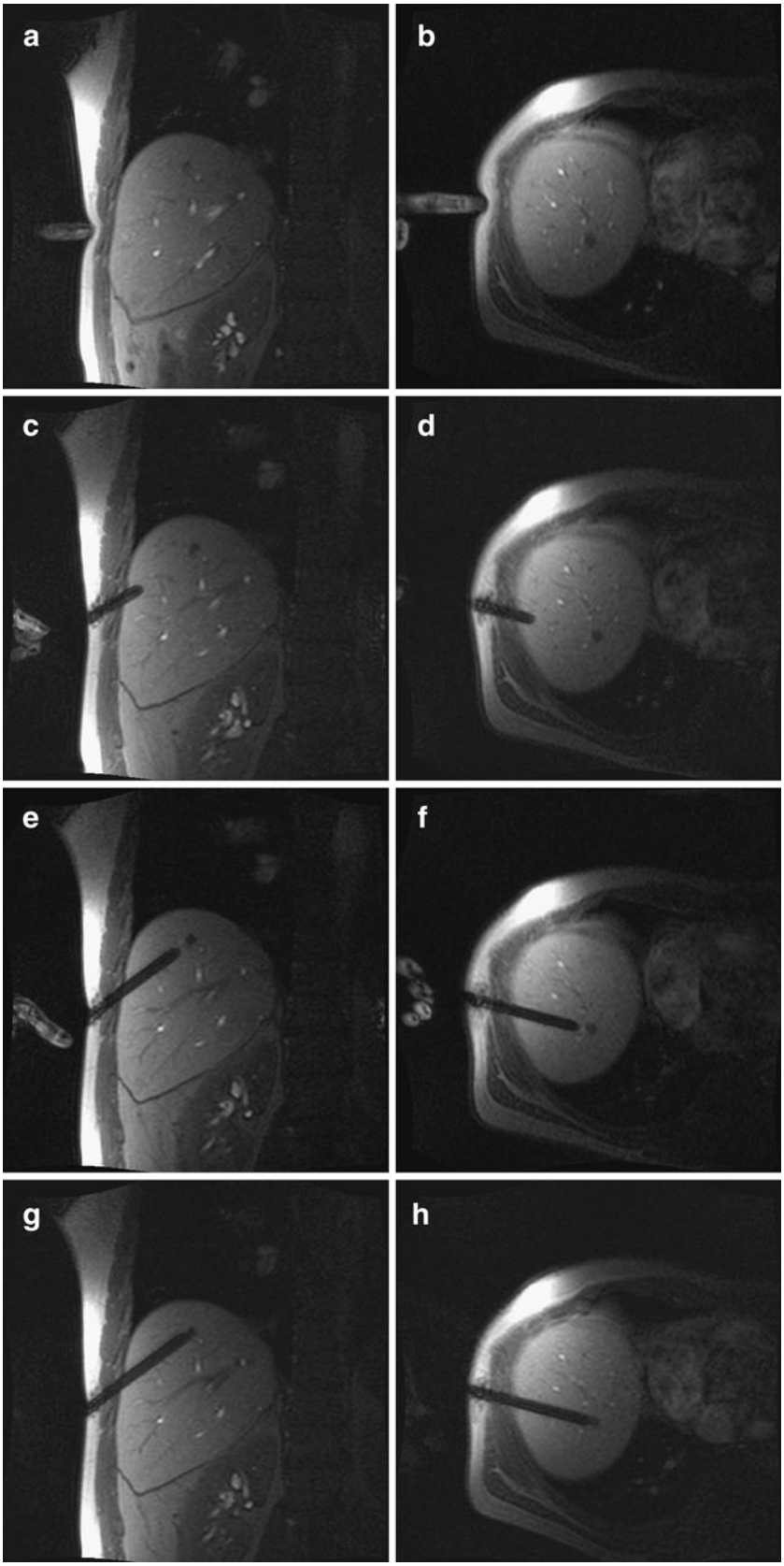

Fig. 1 Gd-EOB-DTPA-enhanced MR fluoroscopy at 1 frame/s showing coronal and paraxial planes used to puncture a lesion measuring <1 cm located in the liver dome. Plane orientations follow the path between needle entry and target. Finger pointing is used to determine the access (**a**, **b**). Images **c**–**h** show the needle progressing towards the lesion. Note the excellent conspicuity of the hypointense lesion in Gd-EOB-DTPA-enhanced liver parenchyma (>20 min post i.v. application)

Institute Common Toxicity Criteria, version 2. Patients underwent a clinical examination and laboratory tests before the first intervention, and at 3 days, 6 weeks and every 3 months post-intervention. At these points in time, imaging procedures were performed including contrast-enhanced MRI (Gd-EOB-DTPA; Primovist, BayerSchering, Germany) and additional abdominal and chest CT upon suspected tumour progression by rising CEA levels or other clinical evidence.

Local tumour control (i.e. stable disease, partial or complete remission) after brachytherapy treatment was determined by contrast-enhanced MRI and defined as either of the following: (1) maximum symmetric increase in the sum of the largest lesion diameter <25% compared with baseline starting at 3 months post-irradiation or (2) absence of asymmetric lesion growth at any time during follow-up. Any suspected tumour recurrence was best differentiated from hepatic parenchyma necrosis on late contrast-enhanced T1w images (20 min. p.i.). Partial response was defined as a lesion volume loss ≥50%, and complete response was defined as lesion disappearance.

Image quality of MR fluoroscopy (T1w FFE) was compared with plain CT imaging acquired ≤ 1 week previous to the interventional procedure. CT images consisted of helical CT with a slice thickness of 5 mm (Toshiba Aquilion 16, Japan). We employed a rating scale for liver-to-lesion contrast from 1 (maximum contrast) to 10 (no visible lesion).

Intervention time was defined as the time interval between the first scout image and the final THRIVE acquisition for treatment planning. Therefore, our definition of intervention time included sterile drape preparation, local anaesthesia, needle positioning, sheath placement and data acquisition for dosimetry planning.

Statistical methods

Differences in lesion conspicuity between CT and MR were evaluated with the Friedman test. Concordance between reviewers was measured with the Kendall's W test. For all tests $P<0.05$ was considered significant. Statistical evaluation was performed using the software package SPSS for Windows.

Results

Patient characteristics

Between February 2008 and February 2009, 104 patients with 224 liver malignancies were treated with MR-guided brachytherapy in 134 sessions. Twenty-one patients presented with HCC, all of them associated with liver cirrhosis, as well as 55 patients with colorectal cancer, 7 patients with breast cancer and 21 patients with other primaries. None of the patients with liver metastases displayed evidence of liver cirrhosis. The mean size of 45 HCC manifestations was 2.1 cm (0.9–5.1 cm), and patients with HCC presented with 1–4 lesions (median: 2 lesions). The mean size of 125 colorectal metastases was 2.3 cm (0.4–9.9 cm), and patients with CRC presented with 1–5 lesions (median: 2 lesions). The mean size of lesions from all other primaries was 1.9 cm (0.5–5.0 cm; 1–4 lesions; median: 1 lesion).

Table 1 lists additional demographic and clinical characteristics of the patients.

Technical success, treatment-related complications and toxicity

On an intention-to-treat basis, the technical success rate was 218 complete ablations in 224 tumours (97%), with complete ablation defined as successful delivery of the intended target dose to the clinical target volume (CTV) (Table 2). In six lesions, we retrospectively encountered deviations of the guide wire position inside the brachytherapy catheter. As the brachytherapy catheter itself was not visible in MR without the nitinol guide wire inside, the catheter position was not visualized properly for brachytherapy planning in these cases, leading to dose delivery outside of the CTV. These technical failures became apparent at first follow-up imaging, with radiation effects to hepatic parenchyma outside the intended CTV. However, countermeasures such as proper fixation of the guide wire were applied after the problem had been identified, and we did not encounter this complication thereafter. We experienced no major complications or severe

Table 1 Demographic and clinical characteristics of the patients (n=104 total patients)

Variable	Results
Age (years)	Mean: 64, range: 49–85
Male sex	65 (68%)
HCC (n=21)	
Child A, B	18 (86%), 3 (14%)
Previous therapies	
TACE	2 (10%)
SIRT	1 (5%)
Nexavar	4 (19%)
Other CTx	1 (5%)
Liver resection	3 (14%)
Local ablation	5 (24%)
CRC (n=55)	
Previous therapies	
Chemotherapy	43 (78%)
Liver resection	24 (44%
Previous local ablation	1 (2%)

HCC Hepatocellular carcinoma, *TACE* transarterial chemoembolization, *SIRT* selective internal radiation therapy, *CTx* chemotherapy, CRC colorectal cancer

Table 2 Treatment characteristics and outcome

Characteristic	Outcome
All patients (n=104)	
No. of catheters (median)	1–5 (1)
Intervention time (mean/median)	63/61 min
Min. dose in CTV (mean/median)	19.6/20.1 Gy
Irradiation time (mean/median)	26.5/25.6 min
Technical failure (n=224 tumours)	6 (2.6%)[a]
Patients/tumours reaching 3 month follow-up	86/166
Local control/assisted local control at 3 months	96%/100%[b]
HCC (n=21)	
Intervention time (mean/median)	58/50 min
Min. dose in CTV (mean/median)	17.1/17.1 Gy
Irradiation time (mean/median)	24.4/25.3 min
CRC (n=55)	
Intervention time (mean/median)	65/62 min
Min. dose in CTV (mean/median)	20.9/21.6 Gy
Irradiation time (mean/median)	28.9/28.8 min

CTV Clinical target volume, *HCC* hepatocellular carcinoma, *CRC* colorectal cancer
[a]Guide wire dislocation preventing appropriate irradiation planning in all six cases
[b]Six lesions were re-irradiated after technical failure

adverse events in 134 interventions in 224 tumours. Minor complications were observed in 5 out of 134 interventions (4%), with nausea and vomiting lasting until 3 days post-intervention in one patient, one asymptomatic subcapsular liver haematoma, one mild allergic reaction, probably to the liver-specific contrast agent used, and one patient each displaying hyper- or hypotonic blood pressure dysregulation during analgosedation, which was treated conservatively and resolved. We encountered no perioperative or 30-day mortality.

We encountered no late complications attributed to the procedure such as post-interventional liver failure by radiation-induced liver disease (RILD) during follow-up.

Image quality and intervention time

The results of the assessment of the image quality on fluoroscopic MR compared with plain CT are displayed in Table 3. Superiority of fluoroscopic, Gd-EOB-DTPA-enhanced images over plain CT was highly significant (P< 0.001) (Fig. 2a, b). Concordance between both reviewers was high (P<0.05). Mean and median intervention times (from first scout acquisition until the final THRIVE sequence) were 64 and 61 min respectively (range 29–174).

Local tumour control

Eighty-six patients treated for 166 liver malignancies reached 3 months' follow-up. The other patients were lost to appropriate MR follow-up. Because of technical failures owing to guide wire dislocation (for visualization of the brachytherapy catheter), we encountered local treatment failures in six patients who underwent re-irradiation after 6–8 weeks. All other tumours displayed local tumour control at 3 months' follow-up. Thus, the primary local control rate was 96%.

Discussion

Minimally invasive oncology has gained increasing interest recently, including numerous new techniques evolving for image-guided local or locoregional tumour ablation. Whereas locoregional approaches usually utilise endovascular access via tumour feeding arteries, local ablative measures most commonly rely on percutaneous interstitial access routes. Treatment success directly correlates with the ability to visualize the target area, and there is a direct correlation between procedural complications and the ability to avoid risk structures when tools and needles are progressed under real-time imaging [9]. In most cases, ultrasound is commonly the imaging method of choice because of its broad availability and real-time capabilities. Alternatively, CT fluoroscopy avoids some of the disadvantages of ultrasound such as image disturbance by intestinal gas or gas bubbles resulting from thermal ablation, or limited access to target areas, e.g. behind ribs, in the liver dome or between bowel loops [10]. On the other hand, CT suffers from comparatively low image contrast during interventional procedures because standard i.v. contrast agents cannot be used. Furthermore, CT is limited to single plane imaging and both the patient and the staff are exposed to radiation [11].

In this study we sought to demonstrate the feasibility and safety of employing an open bore high-field MRI system

Table 3 Image quality assessment for CT and MR fluoroscopy images with two independent reviewers. Rating scale for liver-to-lesion contrast 1–10 (poor to excellent; P<0.001)

	Reviewer 1		Reviewer 2	
	CT plain	MR[a]	CT plain	MR[a]
Median	5	9	5.5	10
Mean	4.7	8.5	4.9	9.4

[a]MR fluoroscopy, 20–60 min p.i. Gd-EOB-DTPA (Primovist)

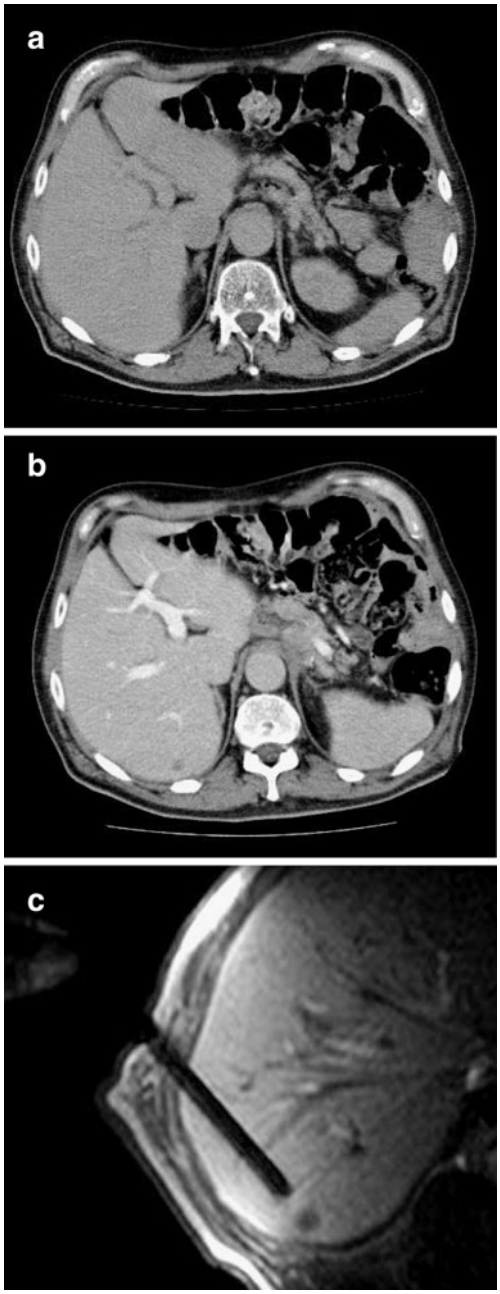

Fig. 2 Negative plain CT (**a**) as it would be used for CT intervention. Contrast-enhanced diagnostic CT confirms a small colorectal liver metastasis (**b**). The corresponding Gd-EOB-DTPA enhanced MR fluoroscopy (**c**) clearly depicts the lesion during the procedure

for interstitial, image-guided intervention of the liver. Within the scope of this research and development project we intended to enhance procedural outcomes through simplified navigation and better tumour conspicuity compared with standard imaging tools such as ultrasound or computed tomography. Image quality exemplified by liver-to-lesion contrast proved to be highly superior compared with CT intervention when applying a hepatocyte-selective contrast agent, and procedural safety and success rates proved to be very high at 3 months' follow-up.

In our system we employed freehand puncture with continuous interactive imaging during near real-time fluoroscopy, with the interventionalist having the choice to toggle between two predefined planes that were usually perpendicular to each other. The technician in the control room selected the path from the skin entry point of the needle to the centre of the target as the starting point. In larger tumours scheduled to receive more than one applicator, the intended peripheral position of each applicator in the target volume was precisely defined before the procedure. During the intervention, the technician diligently modified the orientation of the imaging plane according to needle progress by manually moving a line representing the slice intersection in the graphical user interface of the interactive imaging mode of the MR system.

To avoid loss of orientation in 3D space, the interventionalist concentrated on advancing the needle inside the direct plane between the skin entry and target. If the signal of the needle tip was lost in one plane, correction of the needle orientation was performed in the perpendicular second plane. This approach has some limitations. First, the needle entry point as well as the needle position and orientation have to be identified continuously and the orientation of the imaging plane is adapted manually by the technician (or potentially by the interventionalist using in-room controls) during the ongoing procedure. Second, in cases where there is no direct path from entry point to target (e.g. when taking a biopsy in abdominal locations surrounded by bowel loops), the navigation mode employed is not optimal. In such cases it may be desirable to push the needle underneath a bowel loop, and then lift the bowel by changing the needle angle to gain direct access to the target. In theory, such a procedure may be performed with the navigation mode described if an in-room communication system connecting the interventionalist and the technician is available or if the interventionalist fully navigates the MR by in-room controls. Neither system had been installed at the time of this study.

In the future, we aim to modify navigation under MR fluoroscopy. With the implementation of a newly developed tracking system as part of the ongoing project, the needle orientation manipulated by the interventionalist will automatically define the imaging plane visualized by the MR system. In recent years, numerous technical solutions have been described, ranging from active tracking with catheter-mounted microcoils to fiducial markers mounted in the extracorporeal part of puncture needles. Some of these approaches even employed stereotactic camera systems [26–30]. The technically most demanding and also most rewarding are active coils on catheter tips transmitting a high frequence (HF) signal that can be detected by the MR machine. In principle, this solution requires a

connection between the coil and the MR system, which raises safety concerns of employing a cable inside the magnet [31]. It should also be mentioned that such a solution touches on regulatory issues regarding formal approval of the MR machine as a medical device. Resonant markers mounted on needle or catheter tips have also received some interest in the past. These markers display a strong signal which is detected by the MR system and may be translated into modifications of the plane orientation in time intervals of <1 s [32]. However, resonant markers are usually quite dependent on the orientation in the B_0 field, and their integration into the tip of a puncture needle is not trivial [33]. Whereas both issues may be solved elegantly by extracorporeal markers (at least in the case of puncture needles), this rather pragmatic approach may be hampered by the fact that commercially available MR-compatible needles are not very stiff, and deviations of the theoretical needle tip position during the intervention may occur [28].

Compared with radiofrequency ablation, image-guided brachytherapy has not yet found widespread use, despite its ability to safely and reliably destroy even tumours that are too large for RFA or targets located unfavourably for thermal ablation [23]. In addition, in two recent publications of prospective randomised trials, the method has proven to have a significant prognostic impact on advanced HCC as well as metastatic colorectal carcinoma [34, 35]. MR-compatible tools needed to perform image-guided brachytherapy in MRI are limited to a puncture needle, a polyurethane sheath and a polyurethane brachytherapy catheter. To visualize the brachytherapy catheter we used a guide wire inside shortened to 38 cm (easing safety constraints with respect to a wavelength in tissue of ≈78 cm at 1 Tesla). Guide wires pose a challenge in interventional MRI only if used during imaging inside the magnet since they may induce sparking and heating [36]. Passively marked MR-safe guide wires may represent a valuable alternative [37].

Radiofrequency ablation of liver tumours in MRI has already been demonstrated by numerous other groups. However, most of the techniques described limit themselves to the verification of the (MR-compatible) needle position with the actual intervention, i.e. the ablation procedure, performed outside a cylindrical magnet [15]. Even in publications by groups describing MR fluoroscopic probe positioning for liver tumour ablation, routine use has not yet been achieved for two reasons: first, only an open bore magnet design enables free access to any given tumour location in the liver. Second, RF systems severely interfere with the MR imaging components because of their HF properties. Whereas 1.0T MRI works at 42 MHz, RFA systems such as Rita (Angiodynamics, USA) theoretically emit HF pulses at 460 KHz. In practice, the 93rd harmonic of the 460 KHz pulse will eliminate the MR signal completely if not modulated by a low pass filter. Appropriate filter boxes have been described and are currently being tested by our work group to enable online MR thermometry of radiofrequency ablation of liver tumours [38, 39].

It should be mentioned that as an alternative to MR fluoroscopy, image fusion between plain CT during RFA and preoperative diagnostic MRI may be applied to take advantage of MR superiority in soft tissue contrast. Initial software has been introduced but not yet validated in clinical trials. The clinical performance of contrast-enhanced ultrasound guidance for RFA in comparison to MR-based techniques has also not been evaluated yet.

In summary, the concept of liver ablation employing an open high-field MRI system is feasible and safe. The procedural success rate proved to be very high. The time to perform the interventions remained within reasonable limits. The image quality during MR fluoroscopic intervention was far superior to that of CT. Consequently, we have shifted our indications for image-guided ablation of liver tumours to earlier stages with smaller tumours down to less than 1 cm. We hypothesize that because of limitations in image quality and navigation this would not be possible with CT or ultrasound guidance.

References

1. Goldberg SN, Grassi CJ, Cardella JF et al (2005) Image-guided tumor ablation: standardization of terminology and reporting criteria. J Vasc Interv Radiol 16:765–778
2. Xiao YY, Tian JL, Li JK et al (2008) CT-guided percutaneous chemical ablation of adrenal neoplasms. AJR Am J Roentgenol 190:105–110
3. Gillams AR, Lees WR (2008) Radiofrequency ablation of lung metastases: factors influencing success. Eur Radiol 18(4):672–677
4. Curley SA (2008) Radiofrequency ablation versus resection for resectable colorectal liver metastases: time for a randomized trial? Ann Surg Oncol 15:11–13
5. Zhang YJ, Liang HH, Chen MS et al (2007) Hepatocellular carcinoma treated with radiofrequency ablation with or without ethanol injection: a prospective randomized trial. Radiology 244:599–607
6. Vogl TJ, Straub R, Eichler K et al (2004) Colorectal carcinoma metastases in liver: laser-induced interstitial thermotherapy-local tumor control rate and survival data. Radiology 230:450–458
7. Pech M, Mohnike K, Wieners G, Bialek E, Dudeck O, Seidensticker M, Peters N, Wust P, Gademann G, Ricke J (2008) Radiotherapy of liver metastases. Comparison of target volumes and dose-volume histograms employing CT- or MRI-based treatment planning. Strahlenther Onkol 184:256–261
8. Mast TD, Pucke DP, Subramanian SE, Bowlus WJ, Rudich SM, Buell JF (2008) Ultrasound monitoring of in vitro radio frequency ablation by echo decorrelation imaging. J Ultrasound Med 27:1685–1697

9. Stroszczynski C, Gaffke G (2006) Use of imaging modalities for the guidance of minimally invasive tumor therapies (MITT). Recent Results Cancer Res 167:3–12
10. Nakai M, Sato M, Sahara S, Takasaka I, Kawai N, Minamiguchi H, Tanihata H, Kimura M, Takeuchi N (2009) Radiofrequency ablation assisted by real-time virtual sonography and CT for hepatocellular carcinoma undetectable by conventional sonography. Cardiovasc Intervent Radiol 32:62–69
11. Laganà D, Carrafiello G, Mangini M, Lumia D, Mocciardini L, Chini C, Pinotti G, Cuffari S, Fugazzola C (2008) Hepatic radiofrequency under CT-fluoroscopy guidance. Radiol Med 113:87–100
12. Fahey BJ, Nelson RC, Hsu SJ, Bradway DP, Dumont DM, Trahey GE (2008) In vivo guidance and assessment of liver radio-frequency ablation with acoustic radiation force elastography. Ultrasound Med Biol 34:1590–1603
13. Ricke J, Wust P, Stohlmann A et al (2004) CT-guided interstitial brachytherapy of liver malignancies alone or in combination with thermal ablation: phase I–II results of a novel technique. Int J Radiat Oncol Biol Phys 58:1496–1505
14. Vogl TJ, Müller PK, Hammerstingl R, Weinhold N, Mack MG, Philipp C, Deimling M, Beuthan J, Pegios W, Riess H (1995) Malignant liver tumors treated with MR imaging-guided laser-induced thermotherapy: technique and prospective results. Radiology 196:257–265
15. Gaffke G, Gebauer B, Gnauck M, Knollmann FD, Helmberger T, Ricke J, Oettle H, Felix R, Stroszczynski C (2005) Potential advantages of the MRI for the radiofrequency ablation of liver tumors. Rofo 177:77–83
16. Puls R, Stroszczynski C, Gaffke G, Hosten N, Felix R, Speck U (2003) Laser-induced thermotherapy (LITT) of liver metastases: MR-guided percutaneous insertion of an MRI-compatible irrigated microcatheter system using a closed high-field unit. J Magn Reson Imaging 17:663–670
17. Wacker FK, Reither K, Ritz JP, Roggan A, Germer CT, Wolf KJ (2001) MR-guided interstitial laser-induced thermotherapy of hepatic metastasis combined with arterial blood flow reduction: technique and first clinical results in an open MR system. J Magn Reson Imaging 13:31–36
18. Reither K, Wacker F, Ritz JP, Isbert C, Germer CT, Roggan A, Wendt M, Wolf KJ (2000) Laser-induced thermotherapy (LITT) for liver metastasis in an open 0.2T MRI. Rofo 172:175–178
19. Huppert PE, Trübenbach J, Schick F, Pereira P, König C, Claussen CD (2000) MRI-guided percutaneous radiofrequency ablation of hepatic neoplasms—first technical and clinical experiences. Rofo 172:692–700
20. Lewin JS, Duerk JL, Jain VR, Petersilge CA, Chao CP, Haaga JR (1996) Needle localization in MR-guided biopsy and aspiration: effects of field strength, sequence design, and magnetic field orientation. Am J Roentgenol 166:1337–1345
21. Streitparth F, Gebauer B, Melcher I, Schaser K, Philipp C, Rump J, Hamm B, Teichgräber U (2009) MR-guided laser ablation of osteoid osteoma in an open high-field system (1.0 T). Cardiovasc Intervent Radiol 32:320–325
22. Gossmann A, Bangard C, Warm M, Schmutzler RK, Mallmann P, Lackner KJ (2008) Real-time MR-guided wire localization of breast lesions by using an open 1.0-T imager: initial experience. Radiology 247:535–542
23. Ricke J, Wust P, Wieners G et al (2004) Liver malignancies: CT-guided interstitial brachytherapy in patients with unfavorable lesions for thermal ablation. J Vasc Interv Radiol 15:1279–1286
24. van Montfoort JE, Stieger B, Meijer DK, Weinmann HJ, Meier PJ, Fattinger KE (1999) Hepatic uptake of the magnetic resonance imaging contrast agent gadoxetate by the organic anion transporting polypeptide Oatp1. J Pharmacol Exp Ther 290:153–157
25. Huppertz A, Balzer T, Blakeborough A et al (2004) Improved detection of focal liver lesions at MR imaging: multicenter comparison of gadoxetic acid-enhanced MR images with intraoperative findings. Radiology 230:266–275
26. Zimmermann H, Müller S, Gutmann B, Bardenheuer H, Melzer A, Umathum R, Nitz W, Semmler W, Bock M (2006) Targeted-HASTE imaging with automated device tracking for MR-guided needle interventions in closed-bore MR systems. Magn Reson Med 56:481–488
27. Duerk JL, Wong EY, Lewin JS (2002) A brief review of hardware for catheter tracking in magnetic resonance imaging. MAGMA 13:199–208
28. Weiss CR, Nour SG, Lewin JS (2008) MR-guided biopsy: a review of current techniques and applications. J Magn Reson Imaging 27:311–325
29. Immel E, Melzer A (2006) Improvement of the MR imaging behavior of vascular implants. Minim Invasive Ther Allied Technol 15:85–92
30. Bock M, Wacker FK (2008) MR-guided intravascular interventions: techniques and applications. J Magn Reson Imaging 27:326–338
31. Weiss S, Vernickel P, Schaeffter T, Schulz V, Gleich B (2005) Transmission line for improved RF safety of interventional devices. Magn Reson Med 54:182–189
32. Busse H, Trampel R, Gründer W, Moche M, Kahn T (2007) Method for automatic localization of MR-visible markers using morphological image processing and conventional pulse sequences: feasibility for image-guided procedures. J Magn Reson Imaging 2:1087–1096
33. Will K, Schimpf F, Fischbach F, Ricke J, Schmidt B, Rose G (2010) Pre-tuned resonant marker for iMRI using aerosol deposition on polymer catheters. Proceedings of the SPIE medical imaging conference, 13–18 February 2010, San Diego
34. Mohnike K, Pech M, Seidensticker M, Rühl R, Wieners G, Gaffke G, Kropf S, Felix R, Wust P, Ricke J (2010) Computed-tomography-guided high-dose-rate brachytherapy in hepatocellular carcinoma: safety, efficacy and effect on survival. Int J Radiat Oncol Biol Phys. doi:10.1016/j.ijrobp.2009.07.1700
35. Ricke J, Mohnike K, Pech M, Seidensticker M, Rühl R, Wieners G, Gaffke G, Kropf S, Felix R, Wust P (2010) Local response and impact on survival after local ablation of liver metastases from colorectal carcinoma by CT-guided HDR-brachytherapy. Int J Radiat Oncol Biol Phys. doi:10.1016/j.ijrobp.2009.09.026
36. Buecker A, Spuentrup E, Schmitz-Rode T, Kinzel S, Pfeffer J, Hohl C, van Vaals JJ, Günther RW (2004) Use of a nonmetallic guide wire for magnetic resonance-guided coronary artery catheterization. Invest Radiol 39:656–660
37. Kos S, Huegli R, Hofmann E, Quick HH, Kuehl H, Aker S, Kaiser GM, Borm PJ, Jacob AL, Bilecen D (2009) Feasibility of real-time magnetic resonance-guided angioplasty and stenting of renal arteries in vitro and in swine, using a new polyetheretherketone-based magnetic resonance-compatible guidewire. Invest Radiol 44:234–241
38. Jungnickel K, Gaffke G, Lohfink K, Fischbach F, Bunke J, Will K, Ludewig M, Großer O, Omar A, Ricke J (2009) Evaluation of online thermometry during MR-guided intervention in a high field open system at 1.0 T. Int J CARS 4:S60–S61
39. Seror O, Lepetit-Coiffé M, Le Bail B, de Senneville BD, Trillaud H, Moonen C, Quesson B (2008) Real time monitoring of radiofrequency ablation based on MR thermometry and thermal dose in the pig liver in vivo. Eur Radiol 18:408–416